

Spin polarisation study of NiMnSb using the VCA

H. ALLMAIER^{a,*}, L. CHIONCEL^{a,b}, E. ARRIGONI^a, M. I. KATSNELSON^c, A.I. LICHTENSTEIN^d

^a*Institute of Theoretical Physics, Graz University of Technology, A-8010 Graz, Austria*

^b*Faculty of Science, University of Oradea, RO-47800, Romania*

^c*Institute for Molecules and Materials, Radboud University of Nijmegen, NL-6525 ED Nijmegen, Netherlands*

^d*Institute of Theoretical Physics, University of Hamburg, 20355 Hamburg, Germany*

We investigate the physics of spin polarization in one of the most prominent half-metallic compounds, namely NiMnSb. To this purpose we employ an Nth-order muffin tin orbital (NMTO) based downfolding technique and calculate the electronic structure using a self consistent cluster perturbation technique called variational cluster approach (VCA)

(Received April 1, 2008; accepted June 30, 2008)

Keywords: Spin polarization, NiMnSb, Variation cluster approach

1. Introduction

Since their prediction by de Groot et al.¹ in the early eighties the physics underlying half-metallicity attracted great interest. Ideally, half metallic compounds show metallic behaviour for one spin channel, but isolating behaviour for the opposite. This special property is of high interest in spintronics, a branch of electronics, where not only the charge but also the spin is manipulated. Consequently one would find in a perfect half-metallic ferromagnet a gap in the minority spin channel; however experimentally one never finds 100% spin polarization. Though values as high as 96% (as in CrO₂) are reported, spin polarization is usually significantly lower, more like 40-60%^{2,3} as in the case of NiMnSb. Various reasons are given for this drastic depolarization, like surface and interface effects for $T=0$ depolarization or for finite temperatures correlation effects like the formation of non-quasiparticle states with significant spectral weight at Fermi-energy^{4,5}. For any future use the physics of spin polarization have to be understood.

Future real-world spintronic applications will require in addition operation at room temperature, so compounds with consequently high Curie-temperatures are of interest, like NiMnSb ($T_c=730\text{K}$) or CrO₂ ($T_c=400\text{K}$).

In a previous work⁶ a model Hamiltonian for NiMnSb was presented using the NMTO method where all orbitals except the Mn d-orbitals were downfolded; we continue this work and present here results using a self-consistent cluster perturbation method named variational cluster approach (VCA).

2. NiMnSb

The intermetallic compound *NiMnSb* crystallizes in the cubic structure of *MgAgAs* type ($C1_b$) with the *fcc* Bravais lattice (space group $F43m = T_d^2$). The crystal structure is shown in Fig. 1. This structure can be

described as three interpenetrating *fcc* lattices of *Ni*, *Mn* and *Sb*. The *Ni* and *Sb* sublattices are shifted relative to the *Mn* sublattice by a quarter of the [111] diagonal in opposite directions.

A detailed description of the band structure of semi-Heusler alloys exists using electronic structure calculations and tight-binding model analysis,^{1,7-10} and we briefly summarize the results. The key points which determine the behavior of electrons near the Fermi level for the half-metallic property are the interplay between the crystal structure, valence electron count, covalent bonding and large exchange splitting of the *Mn-d* electrons.

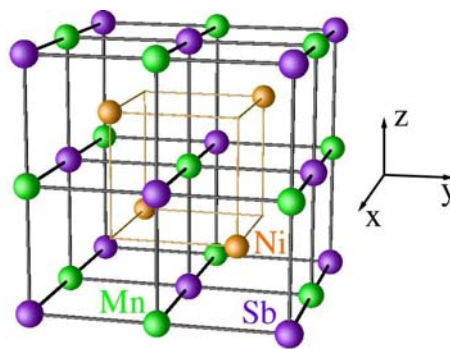


Fig. 1. (Color online) Structure of the semi-Heusler compound NiMnSb: Mn (green) located at $(0,0,0)$ and Sb (purple) located at $(1/2,1/2,1/2)$ form the rock salt structure. Ni (orange) sits at the octahedrally coordinated pocket at one of the cube center positions $(3/4,3/4,3/4)$ and creates holes in the structure by leaving the other $(1/4,1/4,1/4)$ empty.

3. The Variational Cluster Approach (VCA)

The VCA accesses the physics of a lattice model in the thermodynamic limit by optimizing trial self-energies

generated by a reference system. The reference system consists of an isolated cluster having the same interaction as the original lattice, but differing in the single-particle part of the Hamiltonian. The latter can be varied in order to probe the “subspace” spanned by the exact self energies of the reference system as a function of the single particle parameters.

Within the reference system (cluster), the Greens function G_{cl} (which is a matrix in the site and orbital indices) is calculated numerically as a function of frequency and spin, using a zero-temperature Lanczos procedure. Within VCA, one uses the self-energy Σ of the reference system as an approximation to the lattice self-energy, and the corresponding lattice Green’s function G_{VCA} is obtained

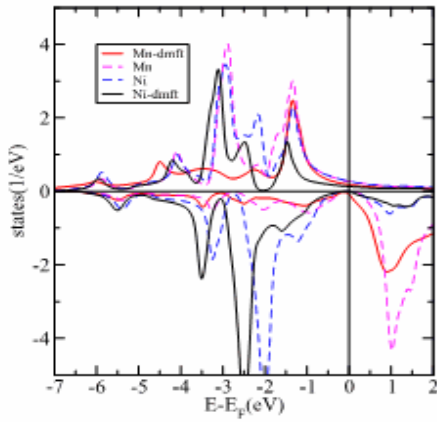


Fig. 2. (Color online) Density of states for NiMnSb using Dynamical Mean field Theory (DMFT)⁵; $U = 3.0\text{eV}$, $J = 0.9\text{eV}$ were used. LSDA-DOS is plotted for comparison.

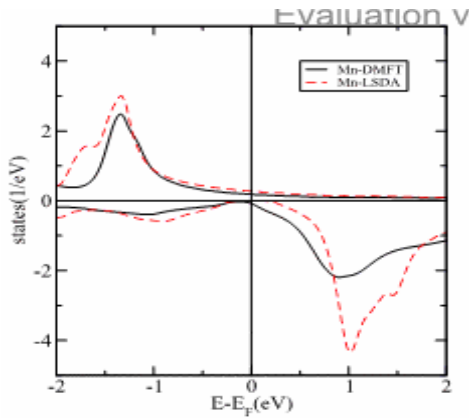


Fig. 3. (Color online) Mn only Density of states obtained from DMFT⁹; $U = 3.0\text{eV}$, $J = 0.9\text{eV}$ were used. LSDA-DOS is plotted for comparison.

by a matrix form of the Dyson equation. The “optimal” self-energy is obtained by finding the saddle point of the SFA potential¹¹

$$\Omega = \Omega' + Tr \ln G_{VCA} - Tr \ln G_d \quad (1)$$

as a function of the single-particle parameters of the reference system. Here, Ω is the grand-canonical potential of the reference system.

Since the reference system is chosen such that memory requirements of the exact diagonalization technique stay within manageable limits, usually not all defined hopping processes can be included within this reference system; however we stress that the remaining hoppings like next nearest neighbour hoppings are not neglected, but taken into account in the noninteracting lattice Green’s function entering the Dyson equation in the expression for the VCA Green’s function.

4. Downfolding onto Mn-d manifolds.

The NMTO method¹²⁻¹⁴ can be used to generate truly minimal basis sets with a massive downfolding technique.

Downfolding produces minimal bands which follows exactly the bands obtained with the full basis set. In a firststep *Mn-d* form the minimal basis set. The truly minimal set of symmetrically orthonormalized NMTOs is a set of Wannier functions. In the construction of the NMTO basis set the active channels are forced to be localized onto the eigenchannel R_{lm} , therefore the NMTO basis set is strongly localized.

Fourier transformation of the orthonormalized NMTO Hamiltonian, $H_{LDA}(k)$, yields on-site energies and hopping integrals,

$$H_{om,Rm}^{LDA} \equiv \langle x_{0m}^\perp | H^{LDA} - \varepsilon_F | x_{Rm}^\perp \rangle \equiv t_{m,m}^{xyz}. \quad (2)$$

in a Wannier representation, where the NMTO Wannier function $|x_{Rm}^\perp\rangle$ is orthonormal

The matrix element between orbitals m' and m , both on site $\mathbf{R}' = \mathbf{R} = \mathbf{0}$, is $t_{m,m'}^{xyz}$, and the hopping integral from orbital m' on site $\mathbf{R}' = \mathbf{0}$ to orbital m on site $\mathbf{R} = (x, y, z)$ is $t_{m,m'}^{xyz}$.

In the many body picture the $Mn_{t_{2g}}$ and e_g constitutes the active orbitals which are responsible for the low energy physics, having fluctuation in occupation and spins.

Further information like the actual matrix elements or technical details of the calculation can be found in the original work⁶.

5. VCA-results

To investigate the correlations in NiMnSb we employed a multi-orbital Hubbard-model

$$H_0 = \sum_{i\{m,\sigma\}} t_{im\sigma,jm'\sigma} c_{im\sigma}^\dagger c_{jm'\sigma} \quad (3)$$

$$H_1 = \frac{1}{2} \sum_{i,m,\sigma} U_{mmmm} n_{im\sigma} n_{im-\sigma} \quad (4)$$

$$+ \frac{1}{2} \sum_{i,m \neq m'} (U_{mm'mm'} - \frac{1}{2} J_{mm'}) n_{im} n_{im'} \quad (5)$$

$$- \sum_{im \neq im'} S_{im} S_{im'}, \quad (6)$$

where $t_{im\sigma, jm'\sigma}$ denotes the coefficient of the hopping process between orbitals m, m' at sites i, j , respectively.

$c_{im\sigma}^\dagger$ and $c_{im\sigma}^\dagger$ are the usual fermionic creation and annihilation operators operating on an electron with spin σ at site i in the orbital m . In this form the Hamiltonian not only includes on-site Coulomb interactions in the same orbital, but between different orbitals, even with different spin orientations, as well; further spin- and pair flip terms are also taken into account.

For the Coulomb interaction we chose intermediate values: $U = 3.0\text{eV}$ and $J = 0.9\text{eV}$, though previous works used values for U ranging from 2 to 4.8 eV^{5,15-17}. The present calculations consider only Mn in the NMTO-basis set; in the real compound also Ni-3d electrons could contribute to the screening of the local Coulomb-interactions. The evaluation of the Coulomb matrix elements is a rather complicated task and beyond the scope of the present paper. By analyzing the band structure by using fat bands, we deduced an average screening factor of 0.4 around Fermi-energy; this leads to the here used reduced values of $U = 0.75$ and $J = 0.23\text{eV}$.

For the VCA calculation we used a simple cluster consisting of two Mn-sites as reference system, as depicted in Fig. 4.

A self consistent calculation was done and the results are presented in Fig.5.

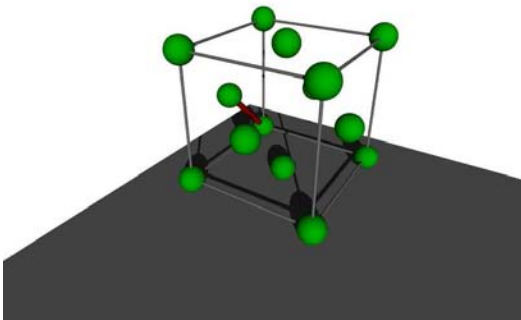


Fig. 4. (color online) Reference system used for the VCA calculation; the red line denotes the used cluster. Note that due to the downfolding procedure only the Mn-sublattice is considered.

Comparing the VCA-DOS with the results from DMFTs in Fig.2 and for the Mn-only DMFT-DOS in Fig.3 one finds significant differences. Due to the down folding onto the Mn-d manifold which is only valid in a small region around Fermi-energy the VCA-results contain no structure at all outside of $[\pm 2\text{ eV}]$.

In a more detailed comparison to the DMFT-results, the VCA-results show vaguely the peak at around -1eV in the majority spin channel, however with considerable more spectral weight for energies between $[-1,0]\text{eV}$. The region above Fermi-energy shows further differences instead of a steady decline - as seen in DMFT and LSDA the VCA with the Mn-only NMTO basis set gives only a small number of states at Fermi-energy and in comparison also more weight above E_F ($[0.5,1]\text{eV}$).

Concerning the minority spin-channel the VCA-results show a significant number of states at roughly -1eV below Fermi-energy, which are not seen to this extent in the DMFT-results.

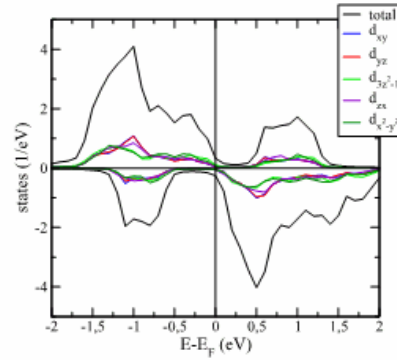


Fig. 5. (Color online) VCA-results for NiMnSb using the Mn only NMTO-basis set; a reduced Coulomb-interaction was used (see text); $U=0.75\text{eV}$, $J=0.9\text{eV}$.

The LSDA-results do show an on-set of states at this position, however these have much less spectral weight in comparison. Above Fermi-energy LSDA shows a peak at about 1eV , which gets flattened in the DMFT. The VCA gives also a peak of reduced spectral weight, albeit far closer to Fermi-energy (about 0.5eV).

We investigated to which extent the limited size of the cluster influences the results, since a significant number of hopping processes are not taken into exact diagonalization. Scaling considerations show however that only the fine structure changes, the general shape stays unmodified to a large extent. Since the general structure of the gathered results shows considerably deficiencies, we argue that this is due to the restriction of the NMTO-basis to only Mn-orbitals.

In addition the downfolding procedure reveals that Ni lies energetically deeper (-3eV to about -1eV), however not so much as to have no influence on the structure at Fermi-energy. Thus, future work has to address this point and include Ni in the NMTO-basis set.

6. Summary

Using the variational cluster approach we have shown that though Mn accounts significantly to the physics at Fermi-energy Ni has to be considered as well to access the complete nature of NiMnSb, even around the Fermi energy. Future work will have to address this point, since this is of special importance for calculations concerning the non-quasiparticle states which are of special interest since they lead to drastic depolarization at finite temperatures.

Acknowledgement

We acknowledge financial support by the Austrian science fund (FWF project P18505-N16).

References

- [1] R. A. de Groot R. A. de Groot, F. M. Mueller, P. G. Engen, K. H. Buschow., *Phys. Rev. Lett.* **50**, 2024 (1983).
- [2] W. R. Branforda et al., *Journal of Magnetism and Magnetic Materials* **272-276**, E1399 (2004).
- [3] R. J. Soulen, Jr., J. M. Byers, M. S. Osofsky, B. Nadgorny, T. Ambrose, S. F. Cheng, P. R. Broussard, C. T. Tanaka, J. Nowak, J. S. Moodera, A. Barry, J. M. D. Coey, *Science* **282**, 85 (1998).
- [4] L. Chioncel, H. Allmaier, E. Arrigoni, A. Yamasaki, M. Daghofer, M. I. Katsnelson, A. I. Lichtenstein, *Phys. Rev. B* **75**, 140406 (2007).
- [5] L. Chioncel, M. I. Katsnelson, R. A. de Groot, A. I. Lichtenstein, *Phys. Rev. B* **68**, 144425 (2003).
- [6] A. Yamasaki, L. Chioncel, A. I. Lichtenstein, O. K. Andersen, *Phys. Rev. B* **74**, 024419 (2006).
- [7] S. Ögüt, K. M. Rabe, *Phys. Rev. B* **104**43 (1995).
- [8] I. Galanakis, P. H. Dederichs, N. Papanikolaou, *Phys. Rev. B* **134**428 (2002).
- [9] B. R. K. Nanda, I. Dasgupta, *J. Phys.: Condens. Matter* **7307** (2003).
- [10] E. Kulatov, I. I. Mazin, *J. Phys.: Condens. Matter* **343** (1990).
- [11] M. Potthoff, *Eur. Phys. J. B* **36**, 335 (2003).
- [12] O. K. Andersen, T. Saha-Dasgupta, *Phys. Rev. B* **R16219** (2000).
- [13] E. Zurek, O. Jepsen, O. K. Andersen, *ChemPhysChem* **1934** (2005).
- [14] O. K. Andersen, O. Jepsen, G. Krier, *World Scientific (Singapore) Methods of Electronic Structure Calculations* **63** (1994).
- [15] L. Chioncel, M. I. Katsnelson, G. A. de Wijs, R. A. de Groot, A. I. Lichtenstein, *Phys. Rev. B* **71**, 085111 (2005).
- [16] L. Chioncel, E. Arrigoni, M. I. Katsnelson, A. I. Lichtenstein, *Phys. Rev. Lett.* **96**, 137203 (2006).
- [17] L. Chioncel, E. Arrigoni, M. I. Katsnelson, A. I. Lichtenstein., *Phys. Rev. Lett.* **96**, 197203 (2006).

*Corresponding author hannes.allmaier@itp.tugraz.at